

<https://doi.org/10.46344/JBINO.2026.v15i01.22>

## MOLECULAR DOCKING-BASED INSIGHTS INTO PYRIMIDINE SCAFFOLD-DERIVED MOIETIES AS POTENTIAL ANTICANCER AGENTS

Mrs.K.Jyothi,Dr.Amit Kumar<sup>1</sup>,Mr.Kokkula Pavan Kumar<sup>2</sup>

\*Research Scholar, Faculty of Pharmaceutical Sciences, Motherhood University, Roorkee, 247661

<sup>1</sup>Research Supervisor, Faculty of Pharmaceutical Sciences, Motherhood University, Roorkee, 247661

<sup>2</sup>Associate Professor, Faculty of Pharmaceutical Sciences, Motherhood University, Roorkee, 247661

### ABSTRACT

Pyrimidine-based heterocycles represent a privileged class of scaffolds in anticancer drug discovery due to their structural similarity to endogenous nucleobases and their proven ability to modulate kinase-driven signaling pathways. In the present study, two series of pyrimidine scaffold-derived moieties, namely pyrimidinyl benzamides (8a–8t) and amide-functionalized pyrimidines (6a–6r), were designed, synthesized, and evaluated through molecular docking studies against key oncogenic kinases, epidermal growth factor receptor (EGFR) and cyclin-dependent kinase-4 (CDK-4). Docking simulations revealed strong and consistent binding affinities of selected derivatives within the ATP-binding pockets of EGFR (PDB ID: 6LUD) and CDK-4 (PDB ID: 7SJ3). Hydrogen bonding,  $\pi$ - $\pi$  stacking, and hydrophobic interactions were identified as the primary stabilizing forces governing ligand-receptor recognition. Electron-donating substituents such as methyl, methoxy, and hydroxy groups significantly enhanced binding affinity, whereas bulky electron-withdrawing groups resulted in reduced interactions. The docking outcomes strongly correlated with reported in vitro cytotoxicity data, supporting the role of kinase inhibition as a plausible mechanism of action. Overall, the study highlights pyrimidine scaffolds as promising candidates for the development of targeted anticancer agents.

**Keywords:** Pyrimidine derivatives; Molecular docking; EGFR; CDK-4; Anticancer agents; Kinase inhibition

## 1.0 Introduction

### 1.1 Cancer: A Global Health Burden

Cancer remains a leading cause of death worldwide, posing a significant challenge to healthcare systems despite continuous advances in diagnosis and therapy. Conventional anticancer treatments such as chemotherapy and radiotherapy are often limited by systemic toxicity, poor selectivity, and the development of drug resistance. Consequently, targeted therapy aimed at specific molecular pathways involved in tumor growth and progression has emerged as an effective strategy in anticancer drug development.

Protein kinases play a central role in regulating cellular processes including proliferation, differentiation, and apoptosis. Dysregulation of kinase signaling pathways is a hallmark of cancer, making kinases attractive therapeutic targets. Among these, cyclin-dependent kinase-4 (CDK-4) is a key regulator of the G1-S phase transition in the cell cycle, while epidermal growth factor receptor (EGFR) is a receptor tyrosine kinase involved in cell growth and survival signaling. Aberrant activation of CDK-4 and EGFR has been implicated in various malignancies, and inhibitors targeting these kinases have shown clinical success.

Pyrimidine scaffolds have gained considerable attention in medicinal chemistry due to their ability to interact with ATP-binding sites of kinases through hydrogen bonding and  $\pi$ - $\pi$  stacking interactions. Numerous clinically approved anticancer drugs incorporate pyrimidine or fused pyrimidine cores, underscoring their pharmacological relevance. Incorporation of a benzamide

moiety further enhances molecular rigidity, hydrogen-bonding capacity, and binding specificity.

Despite extensive research on pyrimidine derivatives, systematic exploration of pyrimidinyl benzamide scaffolds with diverse aryl substitutions remains limited. In this context, the present study focuses on the design, synthesis, molecular docking, and anticancer evaluation of a new series of pyrimidinyl benzamide derivatives (8a-8t) with the aim of identifying potential kinase inhibitors.

### 1.2 Role of Kinases in Cancer Progression

Protein kinases catalyze the transfer of phosphate groups from ATP to specific substrates, thereby modulating intracellular signaling cascades. Dysregulation of kinase activity can lead to uncontrolled cell division and tumorigenesis. Among the numerous kinases implicated in cancer, cyclin-dependent kinases (CDKs) and receptor tyrosine kinases such as epidermal growth factor receptor (EGFR) are of particular importance.

Cyclin-dependent kinase-4 (CDK-4) plays a critical role in regulating the G1-S phase transition of the cell cycle. Overactivation of CDK-4 results in unchecked cell proliferation, a hallmark of cancer. Similarly, EGFR is a transmembrane receptor tyrosine kinase involved in regulating cell growth and survival. Overexpression or mutation of EGFR has been linked to various cancers, including lung, breast, colorectal, and head and neck cancers. Therefore, inhibition of CDK-4 and EGFR has become a well-established strategy in anticancer therapy.

### 1.3 Pyrimidine Scaffold in Anticancer Drug Discovery

Heterocyclic compounds constitute the backbone of many biologically active molecules. Among them, pyrimidine derivatives have gained significant attention in medicinal chemistry due to their wide range of pharmacological activities, including anticancer, antiviral, antimicrobial, anti-inflammatory, and antitubercular properties. Pyrimidines are six-membered aromatic heterocycles containing two nitrogen atoms at positions 1 and 3, which enable strong interactions with biological targets through hydrogen bonding and  $\pi$ - $\pi$  stacking interactions.

The structural similarity of pyrimidines to naturally occurring nucleobases allows them to effectively interact with ATP-binding pockets of kinases. Several clinically approved anticancer drugs, such as CDK inhibitors and EGFR inhibitors, incorporate pyrimidine or fused pyrimidine cores, underscoring their therapeutic relevance. The ease of functionalization at different positions of the pyrimidine ring further enhances their suitability as lead scaffolds in anticancer drug discovery.

### 1.4. Importance of Molecular Docking in Anticancer Drug Discovery

The discovery and development of effective anticancer agents is a complex and resource-intensive process, largely due to the molecular heterogeneity of cancer and the involvement of multiple dysregulated signaling pathways. In this context, molecular docking has emerged as a powerful computational tool that enables the prediction of ligand-protein interactions at the atomic level, providing

valuable insights into the binding affinity, orientation, and interaction patterns of small molecules with biological targets. Molecular docking plays a critical role in structure-based drug design, particularly for kinase-driven cancers, where aberrant activation of proteins such as epidermal growth factor receptor (EGFR) and cyclin-dependent kinases (CDKs) contributes to uncontrolled cell proliferation and tumor progression. By simulating the binding of small molecules within the active sites of target proteins, docking studies facilitate the identification of key molecular interactions—such as hydrogen bonding,  $\pi$ - $\pi$  stacking, hydrophobic contacts, and electrostatic forces—that govern inhibitory activity.

One of the major advantages of molecular docking is its ability to prioritize lead compounds from large libraries of synthesized or virtual molecules, thereby significantly reducing experimental cost, time, and labor. Docking analysis aids in the rational optimization of chemical structures by correlating substituent effects with binding efficiency, enabling the establishment of structure-activity relationships (SAR) before extensive biological evaluation. This is particularly valuable in anticancer research, where selectivity toward tumor-associated targets over normal cellular proteins is essential to minimize toxicity.

Furthermore, molecular docking provides mechanistic insights that complement *in vitro* and *in vivo* studies. The correlation between docking scores and experimental cytotoxicity data strengthens confidence in the proposed mechanism of action and supports target-specific inhibition. In the case of

pyrimidine-based scaffolds, which are structurally analogous to endogenous nucleobases and known for their kinase-binding potential, docking studies are instrumental in validating their suitability as anticancer pharmacophores.

Overall, molecular docking serves as a bridge between synthetic chemistry and biological evaluation, guiding rational drug design and accelerating the identification of promising anticancer candidates. Its integration with experimental approaches represents a modern and efficient strategy for the development of targeted anticancer therapeutics.

## Literature Review

### 2.1 Pyrimidine-Based Compounds as Anticancer Agents

Extensive research has demonstrated the therapeutic importance of pyrimidine derivatives in anticancer drug development. Various substituted pyrimidines and fused pyrimidine systems have shown potent inhibitory activity against kinases involved in cancer progression. Literature reports indicate that pyrimidine scaffolds can be effectively modified to target specific kinases with high selectivity.

Several studies have highlighted the ability of pyrimidine derivatives to inhibit CDKs, EGFR, MNK1, HER2, and other oncogenic kinases. These compounds often exhibit strong correlation between molecular docking predictions and experimental anticancer activity, emphasizing the value of structure-based drug design approaches.

### 2.2 Molecular Docking in Anticancer Drug Design

Molecular docking has become an indispensable tool in modern drug discovery, particularly in anticancer research. Docking studies provide insights into ligand–protein interactions, binding modes, and affinity, thereby aiding in the rational design of potent inhibitors. In the context of pyrimidine derivatives, docking studies have been extensively used to predict binding to kinase targets and to rationalize observed biological activity.

Numerous reports demonstrate that pyrimidine derivatives exhibiting strong docking scores and stable hydrogen-bond interactions often translate into potent kinase inhibition. Therefore, molecular docking was employed in the present study as a primary tool to evaluate the anticancer potential of the synthesized pyrimidine derivative.

Alamshany et al. (2023) reported the synthesis of novel pyrido[2,3-d]pyrimidine, tetrazolo[1,5-c]pyrimidine, and pyrido[3,2-e][1,3,4]triazolo derivatives through diverse chemical transformations starting from intermediate 3b. The structures of the synthesized compounds were confirmed using spectroscopic techniques and elemental analysis. Molecular docking studies were performed using AutoDock Vina to evaluate antiviral activity against the SARS-CoV-2 main protease (Mpro). Compounds 7c, 7d, and 7e exhibited significant antiviral potential with  $IC_{50}$  values of 1.2, 2.34, and 2.3  $\mu$ M, respectively, outperforming the reference drug lopinavir. The strong correlation between in vitro and in silico results highlighted the therapeutic potential of pyrimidine-based heterocycles.

Ramesh et al. (2023) synthesized two series of novel multifunctional pyrimidine–

imine hybrids and evaluated their antimicrobial and antitubercular activities. Several compounds demonstrated significant in vitro antitubercular potency, with compound D16 exhibiting a  $MIC_{100}$  value of 6  $\mu$ M, comparable to the standard drug ethambutol ( $MIC_{100} = 7.63 \mu$ M). Compounds D20, D19, D18, D12, and D7 also showed notable activity with  $MIC_{100}$  values ranging from 10.60 to 50.86  $\mu$ M. Importantly, the synthesized compounds were non-cytotoxic at 25  $\mu$ g/mL in the murine macrophage cell line (RAW 264.7). Additionally, compound M9 displayed moderate to excellent antibacterial and anticandidal activity. Molecular docking studies against *Mycobacterium tuberculosis* thymidylate kinase were performed to elucidate the probable mechanism of action and binding interactions of the compounds.

### 3.0 Materials and Methods

#### 3.1 Ligand Dataset

Two series of pyrimidine derivatives synthesized and characterized experimentally were selected for docking studies:

##### 3.1.1 Multicomponent Synthesis of Di-Substituted Pyrimidine

The di-substituted pyrimidine intermediate 2-(4-methylpyrimidin-5-yl)acetonitrile (4) was synthesized via a multicomponent reaction. A substituted enamine (1.0 equiv, 10 mmol), ortho ester (3.0 equiv, 30

mmol), and ammonium acetate (3.0 equiv, 20 mmol) were refluxed in benzene or toluene at 70–80 °C in the presence of a Lewis acid catalyst, zinc chloride or aluminum chloride. The progress of the reaction was monitored by thin-layer chromatography (TLC) under UV light. Upon completion, the reaction mixture was cooled and subjected to basic work-up using saturated sodium bicarbonate solution. The crude product was extracted, concentrated, and purified by column chromatography using ethyl acetate : hexane (1:9 v/v) as the mobile phase. The purified intermediate was further recrystallized from ethanol to afford the desired pyrimidine derivative (Suzuki et al., 2007; Stanovnik&Svete, 2004; Sakai et al., 2006; Konakahara et al., 2005).

##### 3.1.2 Synthesis of 2-(4-Methylpyrimidin-5-yl)ethan-1-amine (5)

The nitrile intermediate 2-(4-methylpyrimidin-5-yl)acetonitrile (4) was reduced to the corresponding primary amine under inert conditions. A flame-dried 25 mL round-bottom flask equipped with a magnetic stirrer was charged with compound 4 (1.0 mmol) dissolved in anhydrous tetrahydrofuran (THF, 10 mL) and cooled to 0 °C using an ice bath. Lithium aluminum hydride ( $LiAlH_4$ , 3.0 equiv, 114 mg) was added portionwise over 10 min to control exothermicity.

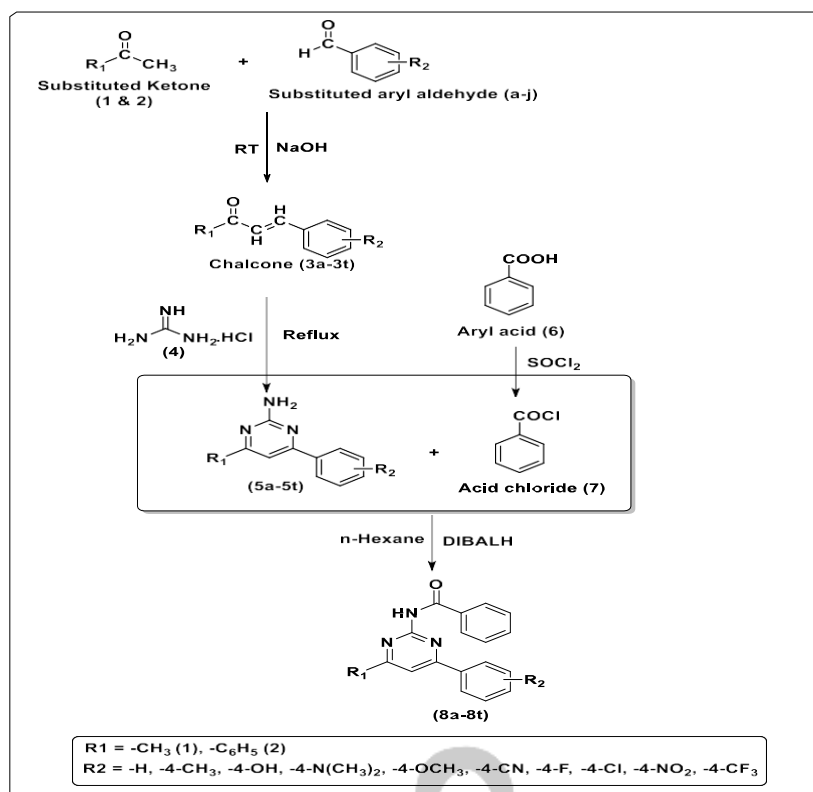


**Figure: Scheme of synthesis of substituted pyrimidinyl benzamides**

The reaction mixture was allowed to warm to room temperature and stirred for 3 h, with progress monitored by TLC ( $CH_2Cl_2/MeOH$ , 9:1). Upon completion, the reaction was carefully quenched at 0 °C by sequential dropwise addition of water (0.1 mL), 15% aqueous NaOH (0.1 mL), and additional water (0.3 mL), followed by stirring for 15 min. The mixture was filtered through a Celite pad, washed with THF (3 × 5 mL), and concentrated under reduced pressure. The crude product was purified by flash chromatography ( $SiO_2$ ,  $CH_2Cl_2/MeOH/NH_4OH$ , 90:9:1) to afford **2-(4-methylpyrimidin-5-yl)ethan-1-amine (5)** as a solid (House, 1972; Larock, 1999).

### 3.1.3 General Procedure for the Synthesis of Amide-Functionalized Pyrimidine Derivatives (6a–6r)

Amide-functionalized pyrimidine derivatives (6a–6r) were synthesized via DCC/DMAP-mediated coupling. The appropriate carboxylic acid (a–r) (1.0 mmol, 1.0 equiv) was dissolved in dry dichloromethane (DCM, 10 mL) in a reaction flask equipped with a magnetic stirrer and cooled in an ice bath. N,N'-dicyclohexylcarbodiimide (DCC, 1.2 equiv) was added, and the mixture was stirred for 15–30 min. Subsequently, 4-dimethylaminopyridine (DMAP, 0.1 equiv) was added, followed by slow addition of the primary amine intermediate **5** (1.0 equiv) under continued cooling.

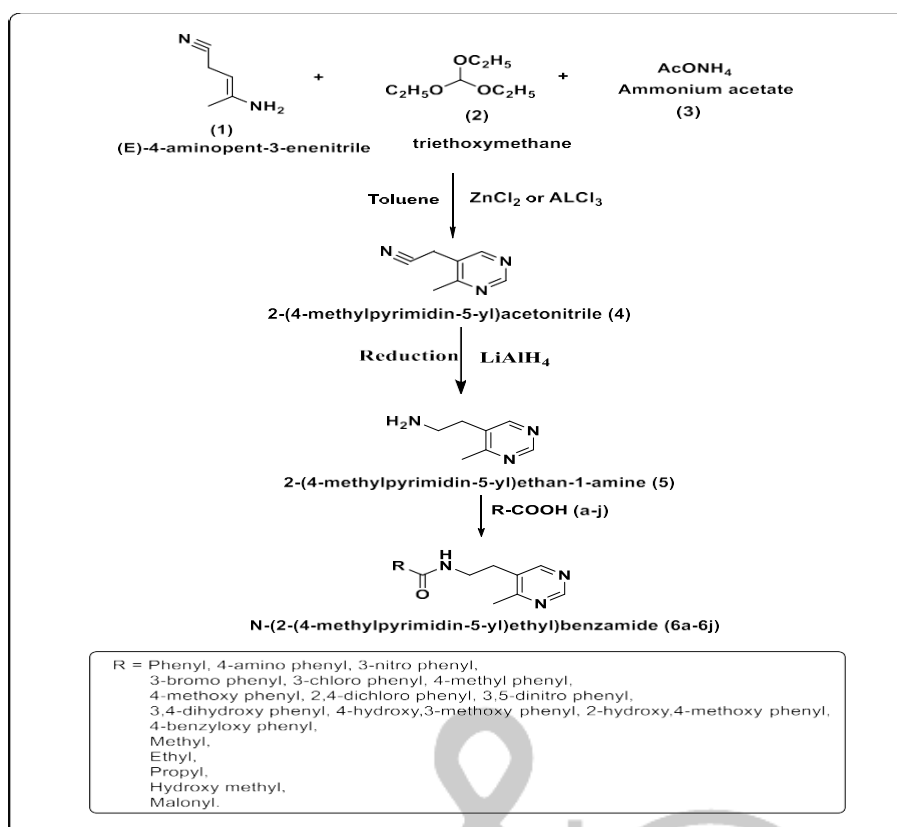


**Figure: Scheme of Synthesis for the amide functionalized pyrimidine derivatives 6a-6j**

The reaction mixture was allowed to warm gradually to room temperature and stirred for 18 h, with reaction progress monitored by TLC. Upon completion, the reaction was quenched with water (10 mL) and extracted with DCM (3 × 20 mL). The combined organic layers were washed successively with saturated sodium bicarbonate solution (2 × 20 mL) and brine (20 mL), dried over anhydrous magnesium sulfate ( $\text{MgSO}_4$ ), filtered, and concentrated under reduced pressure. The crude product was purified by column chromatography on silica gel using hexane : ethyl acetate (8:2 v/v) as the eluent to obtain the desired amide-functionalized pyrimidine derivatives (Meng et al., 2011).

All ligands were geometry-optimized prior to docking.

### 3.2 Protein Preparation

The crystal structures of the epidermal growth factor receptor (EGFR) kinase domain (PDB ID: 6LUD) and cyclin-dependent kinase-4 (CDK-4) (PDB ID: 7SJ3) were retrieved from the Protein Data Bank. Protein preparation was carried out using the Protein Preparation Wizard in the Schrödinger suite. All crystallographic water molecules, ions, and co-crystallized ligands were removed to prevent interference with ligand binding. Missing hydrogen atoms were added, bond orders were assigned, and appropriate protonation states were generated at physiological pH. The prepared protein structures were subsequently subjected to restrained energy minimization using the OPLS-2005 force field to relieve steric clashes and optimize geometry prior to molecular docking.

### 3.3 Docking Protocol

Ligand preparation was performed using the LigPrep module of the Schrödinger suite with geometry optimization carried out under the OPLS-2005 force field. Appropriate ionization states were generated at physiological pH, and low-energy conformations were retained for docking. The receptor grid was generated around the ATP-binding site using the SiteMap tool. Molecular docking was conducted using the Glide extra-precision (XP) mode, and docked conformations were ranked based on Glide score (kcal/mol). The binding modes and key ligand-protein interactions were analyzed using Maestro visualization tools.

### 3.4 Analytical Characterization

#### 3.4.1 Physical Properties of Synthesized Compounds

All synthesized compounds were obtained as crystalline solids with distinct physical appearances. The pyrimidinyl benzamide derivatives (8a–8t) were generally isolated as pale yellow, off-white, or white solids, whereas the amide-functionalized pyrimidine derivatives (6a–6r) appeared as white to light brown solids depending on the nature of the substituents.

#### Pyrimidinyl Benzamide Derivatives (8a–8t): Physical Appearance

8a: *N*-(4-Methyl-6-phenylpyrimidin-2-yl)benzamide — Pale yellow solid  
 8b: *N*-(4-Methyl-6-(*p*-tolyl)pyrimidin-2-yl)benzamide — Pale yellow solid  
 8c: *N*-(4-(4-Hydroxyphenyl)-6-methylpyrimidin-2-yl)benzamide — Pale yellow solid  
 8d: *N*-(4-(4-(Dimethylamino)phenyl)-6-methylpyrimidin-2-yl)benzamide — Pale yellow solid

8e: *N*-(4-(4-Methoxyphenyl)-6-methylpyrimidin-2-yl)benzamide — Pale yellow solid  
 8f: *N*-(4-(4-Cyanophenyl)-6-methylpyrimidin-2-yl)benzamide — Pale yellow solid  
 8g: *N*-(4-(4-Fluorophenyl)-6-methylpyrimidin-2-yl)benzamide — Pale yellow solid  
 8h: *N*-(4-(4-Chlorophenyl)-6-methylpyrimidin-2-yl)benzamide — Off-white solid  
 8i: *N*-(4-Methyl-6-(4-nitrophenyl)pyrimidin-2-yl)benzamide — Pale brown solid  
 8j: *N*-(4-Methyl-6-(4-(trifluoromethyl)phenyl)pyrimidin-2-yl)benzamide — Pale yellow solid  
 8k: *N*-(4,6-Diphenylpyrimidin-2-yl)benzamide — Pale yellow solid  
 8l: *N*-(4-Phenyl-6-(*p*-tolyl)pyrimidin-2-yl)benzamide — Pale yellow solid  
 8m: *N*-(4-(4-Hydroxyphenyl)-6-phenylpyrimidin-2-yl)benzamide — Pale yellow solid  
 8n: *N*-(4-(4-(Dimethylamino)phenyl)-6-phenylpyrimidin-2-yl)benzamide — Pale yellow solid  
 8o: *N*-(4-(4-Methoxyphenyl)-6-phenylpyrimidin-2-yl)benzamide — White solid  
 8p: *N*-(4-(4-Cyanophenyl)-6-phenylpyrimidin-2-yl)benzamide — Pale yellow solid  
 8q: *N*-(4-(4-Fluorophenyl)-6-phenylpyrimidin-2-yl)benzamide — Pale yellow solid  
 8r: *N*-(4-(4-Chlorophenyl)-6-phenylpyrimidin-2-yl)benzamide — White solid  
 8s: *N*-(4-(4-Nitrophenyl)-6-phenylpyrimidin-2-yl)benzamide — Pale brown solid  
 8t: *N*-(4-Phenyl-6-(4-(trifluoromethyl)phenyl)pyrimidin-2-

yl)benzamide — Pale yellow solid

### Amide-Functionalized Pyrimidine Derivatives (6a–6r): Physical Appearance

6a: *N*-(2-Hydroxyphenyl)-2-(4-methylpyrimidin-5-yl)acetamide — White solid

6b: *N*-(3-Hydroxyphenyl)-2-(4-methylpyrimidin-5-yl)acetamide — Off-white solid

6c: *N*-(4-Hydroxyphenyl)-2-(4-methylpyrimidin-5-yl)acetamide — White solid

6d: *N*-(2-Nitrophenyl)-2-(4-methylpyrimidin-5-yl)acetamide — Pale yellow solid

6e: *N*-(3-Nitrophenyl)-2-(4-methylpyrimidin-5-yl)acetamide — Pale yellow solid

6f: *N*-(4-Nitrophenyl)-2-(4-methylpyrimidin-5-yl)acetamide — Yellow solid

6g: *N*-(2-Methoxyphenyl)-2-(4-methylpyrimidin-5-yl)acetamide — Off-white solid

6h: *N*-(3-Methoxyphenyl)-2-(4-methylpyrimidin-5-yl)acetamide — White solid

6i: *N*-(4-Methoxyphenyl)-2-(4-methylpyrimidin-5-yl)acetamide — White solid

6j: *N*-(3,4-Dihydroxyphenyl)-2-(4-methylpyrimidin-5-yl)acetamide — Light brown solid

6k: *N*-(4-Hydroxy-3-methoxyphenyl)-2-(4-methylpyrimidin-5-yl)acetamide — Light brown solid

6l: *N*-(2-Hydroxy-4-methoxyphenyl)-2-(4-methylpyrimidin-5-yl)acetamide — Light brown solid

6m: *N*-(4-Benzyloxyphenyl)-2-(4-methylpyrimidin-5-yl)acetamide — Off-white solid

6n: *N*-(4-Dimethylaminophenyl)-2-(4-methylpyrimidin-5-yl)acetamide — Pale

yellow solid

6o: *N*-(4-Ethylphenyl)-2-(4-methylpyrimidin-5-yl)acetamide — White solid

6p: *N*-(4-Propylphenyl)-2-(4-methylpyrimidin-5-yl)acetamide — White solid

6q: *N*-(4-Butylphenyl)-2-(4-methylpyrimidin-5-yl)acetamide — White solid

6r: *N*-(Malonyl)-2-(4-methylpyrimidin-5-yl)acetamide — Off-white solid

## 4.0 Results and Discussion

### 4.1 Structural Confirmation and Chemical Integrity

All synthesized pyrimidine scaffold-derived moieties were obtained in good to excellent yields, demonstrating the robustness and reproducibility of the adopted synthetic strategies. Structural confirmation of the pyrimidinyl benzamide derivatives was primarily established through  $^1\text{H}$  and  $^{13}\text{C}$  NMR spectroscopy. The appearance of a characteristic singlet in the range of  $\delta$  9.5–9.8 ppm in the  $^1\text{H}$  NMR spectra of the final compounds corresponds to the amide ( $-\text{CONH}-$ ) proton, confirming successful amide bond formation. Additionally, the  $^{13}\text{C}$  NMR spectra displayed carbonyl carbon resonances in the region of  $\delta$  160–170 ppm, further validating the presence of the benzamide functionality.

Similarly, amide-functionalized pyrimidine derivatives exhibited well-resolved spectral signals consistent with their proposed structures. These spectroscopic features collectively confirm the successful synthesis and chemical integrity of the designed pyrimidine scaffolds.

## 4.2 Molecular Docking Analysis against EGFR

Docking studies against the EGFR kinase domain revealed that the pyrimidinyl benzamide derivatives effectively occupied the ATP-binding pocket of the receptor. Compounds bearing electron-donating substituents on the phenyl ring demonstrated superior binding affinity, as evidenced by favorable docking scores and stable interaction profiles.

The pyrimidine nitrogen atoms played a crucial role in anchoring the ligands through hydrogen bonding with key active-site residues, while aromatic rings participated in  $\pi$ - $\pi$  stacking interactions that enhanced complex stability. Hydrophobic substituents further strengthened ligand-protein interactions by occupying lipophilic regions within the binding cavity. In contrast, bulky electron-withdrawing groups resulted in suboptimal orientation and weaker binding affinity, indicating steric and electronic incompatibility with the EGFR active site.

Molecular docking of the synthesized pyrimidine-based amide derivatives (6a–

**Table:** Molecular docking scores (kcal/mol) of amide-functionalized pyrimidine derivatives (6a–6r) against EGFR (PDB ID: 6LUD) and CDK-4 (PDB ID: 7SJ3), along with the reference inhibitors Osimertinib (EGFR) and Abemaciclib (CDK-4)

Compound	R1	Target	
		EGFR(6LUD)	CDK-4(7SJ3)
6a	Phenyl	-5.811	-5.727
6b	2-hydroxyphenyl	-6.957	-8.45
6c	3-nitrophenyl	-5.098	-6.225
6d	3-bromophenyl	-6.704	-6.061

6r) against the EGFR tyrosine kinase domain (PDB ID: 6LUD) yielded docking scores ranging from -4.993 to -7.245 kcal/mol, indicating moderate to strong binding affinities. Compound 6k (4-hydroxy-3-methoxyphenyl) exhibited the highest affinity (-7.245 kcal/mol), followed closely by 6j (3,4-dihydroxyphenyl, -7.215 kcal/mol) and 6b (2-hydroxyphenyl, -6.957 kcal/mol). These results highlight the favorable role of hydroxyl and methoxy substituents, which likely enhance binding through hydrogen bonding and electrostatic interactions within the EGFR ATP-binding pocket. In contrast, compounds bearing bulky or electron-withdrawing groups showed reduced affinity; notably, 6m (4-benzyloxyphenyl) and 6c (3-nitrophenyl) exhibited weaker binding, possibly due to steric hindrance and unfavorable electronic effects. Overall, the docking results underscore the importance of polar, hydrogen bond-donating groups for effective EGFR binding and provide valuable guidance for further SAR-driven optimization.

<b>6e</b>	3-chlorophenyl	-6.544	-5.998
<b>6f</b>	4-methylphenyl	-5.492	-7.959
<b>6g</b>	4-methoxyphenyl	-6.059	-5.96
<b>6h</b>	2,4-dichlorophenyl	-6.112	-6.621
<b>6i</b>	3,5-dinitrophenyl	-5.368	-5.82
<b>6j</b>	3,4-dihydroxyphenyl	-7.215	-8.72
<b>6k</b>	4-hydroxy,3-methoxyphenyl	-7.245	-6.919
<b>6l</b>	2-hydroxy,4-methoxyphenyl	-6.884	-9.23
<b>6m</b>	4-benzyloxyphenyl	-4.993	-6.675
<b>6n</b>	Methyl	-5.763	-6.352
<b>6o</b>	Ethyl	-5.839	-6.635
<b>6p</b>	Propyl	-5.961	-6.745
<b>6q</b>	Hydroxymethyl	-6.623	-6.016
<b>6r</b>	Malonyl	-6.03	-7.896

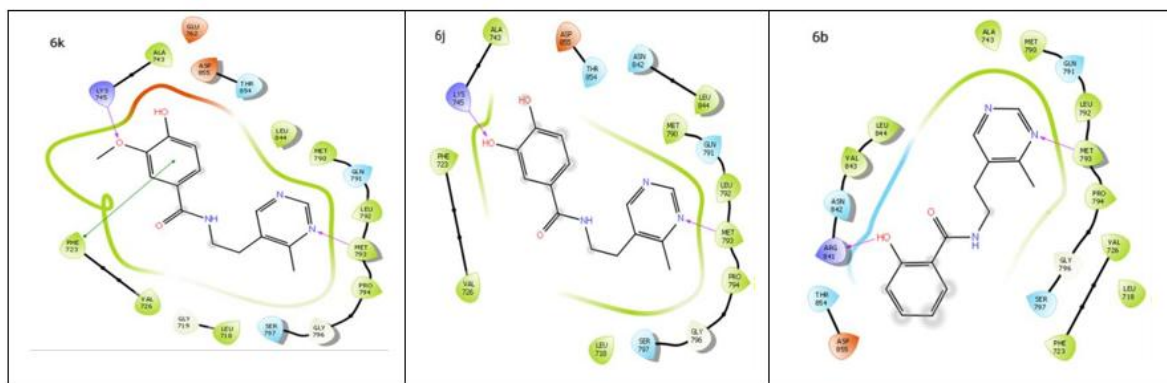


**Figure :** Interactions of Compounds 6k, 6j and 6b at the active site of EGFR (6LUD) protein

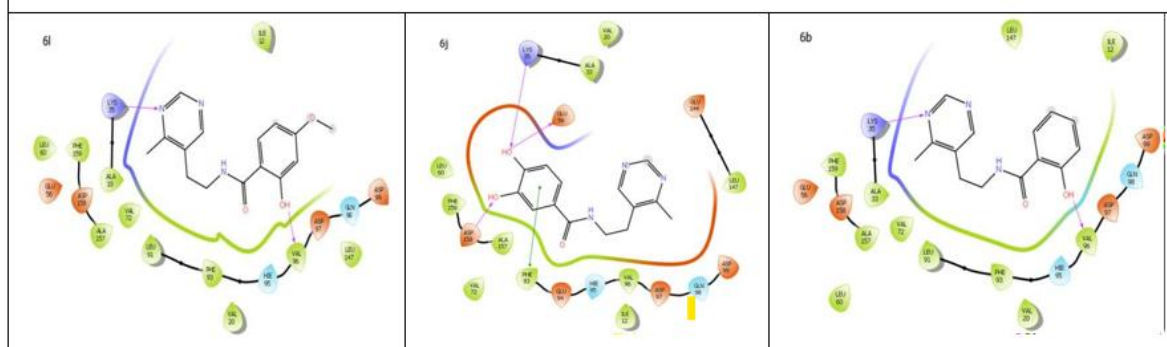


**Figure :** Interactions of Compounds 6l, 6j and 6b at the active site of CDK-4 (7SJ3) protein

### 4.3 Molecular Docking Analysis against CDK-4

The amide-functionalized pyrimidine derivatives exhibited enhanced affinity toward the CDK-4 binding pocket compared to the benzamide series. Hydroxy- and methoxy-substituted derivatives showed the most favorable docking scores, forming multiple hydrogen bonds with catalytically important amino acid residues.

The amide linker contributed significantly to ligand stabilization by enabling proper alignment of the pyrimidine core within the catalytic cleft. Electron-withdrawing substituents, particularly nitro and cyano groups, negatively impacted binding affinity by reducing hydrogen-bonding potential and introducing steric hindrance.

The docking scores of the pyrimidinyl benzamide derivatives (8a–8t) against

CDK-4 (PDB ID: 7SJ3) ranged from  $-8.254$  to  $-4.883$ , indicating variable binding affinities influenced by substituent effects. Among the series, compound 8c ( $-8.254$ ,  $R_2$ : 4-OH) exhibited the highest binding affinity, suggesting strong ligand–protein interactions, likely supported by hydrogen bonding. Compounds 8a, 8f, 8g, 8h, 8i, and 8j showed moderate affinity, whereas 8e and compounds 8k–8t displayed comparatively lower binding energies. Overall, derivatives bearing electron-donating substituents, particularly hydroxyl and methoxy groups, demonstrated enhanced affinity toward 7SJ3, whereas electron-withdrawing groups such as fluoro, chloro, nitro, and cyano substituents resulted in reduced binding.

Within the phenyl-substituted series (8k–8t), compound 8m ( $-6.925$ ,  $R_2$ : 4-OH) showed the strongest affinity, reinforcing

the favorable role of hydroxyl substitution in stabilizing ligand–protein interactions. Compounds 8r, 8t, and 8s exhibited moderate affinity, while compound 8l (-4.214, R<sub>2</sub>: 4-CH<sub>3</sub>) also demonstrated appreciable binding, indicating that both electronic and steric factors influence CDK-4 binding. Comparative analysis

against EGFR (6LUD) and CDK-4 (7SJ3) revealed target-specific binding behavior, with electron-donating substituents generally favoring CDK-4 inhibition, whereas electron-withdrawing groups showed weaker interactions with both targets.

**Table:** Molecular docking scores (kcal/mol) of pyrimidinyl benzamide derivatives (8a–8t) against EGFR (PDB ID: 6LUD) and CDK-4 (PDB ID: 7SJ3), along with the reference inhibitors Osimertinib (EGFR) and Abemaciclib (CDK-4)

Compoundid	R1	R2	DockingScores	
			6LUD	7SJ3
8a	-CH <sub>3</sub>	-H	-5.428	-6.402
8b	-CH <sub>3</sub>	-4-CH <sub>3</sub>	-6.442	-6.352
8c	-CH <sub>3</sub>	-4-OH	-4.939	-8.254
8d	-CH <sub>3</sub>	-4-N(CH <sub>3</sub> ) <sub>2</sub>	-5.967	-5.976
8e	-CH <sub>3</sub>	-4-OCH <sub>3</sub>	-5.45	-7.019
8f	-CH <sub>3</sub>	-4-CN	-5.589	-4.883
8g	-CH <sub>3</sub>	-4-F	-4.201	-6.657
8h	-CH <sub>3</sub>	-4-Cl	-5.877	-5.738
8i	-CH <sub>3</sub>	-4-NO <sub>2</sub>	-4.099	-5.461
8j	-CH <sub>3</sub>	-4-CF <sub>3</sub>	-4.11	-5.718
8k	-C <sub>6</sub> H <sub>5</sub>	-H	-3.918	-4.863
8l	-C <sub>6</sub> H <sub>5</sub>	-4-CH <sub>3</sub>	-2.665	-4.214
8m	-C <sub>6</sub> H <sub>5</sub>	-4-OH	-5.397	-6.925
8n	-C <sub>6</sub> H <sub>5</sub>	-4-N(CH <sub>3</sub> ) <sub>2</sub>	-3.002	-5.363
8o	-C <sub>6</sub> H <sub>5</sub>	-4-OCH <sub>3</sub>	-3.647	-3.817
8p	-C <sub>6</sub> H <sub>5</sub>	-4-CN	-3.183	-6.348
8q	-C <sub>6</sub> H <sub>5</sub>	-4-F	-3.581	-6.105
8r	-C <sub>6</sub> H <sub>5</sub>	-4-Cl	-3.902	-4.956
8s	-C <sub>6</sub> H <sub>5</sub>	-4-NO <sub>2</sub>	-3.445	-4.717
8t	-C <sub>6</sub> H <sub>5</sub>	-4-CF <sub>3</sub>	-4.055	-4.845

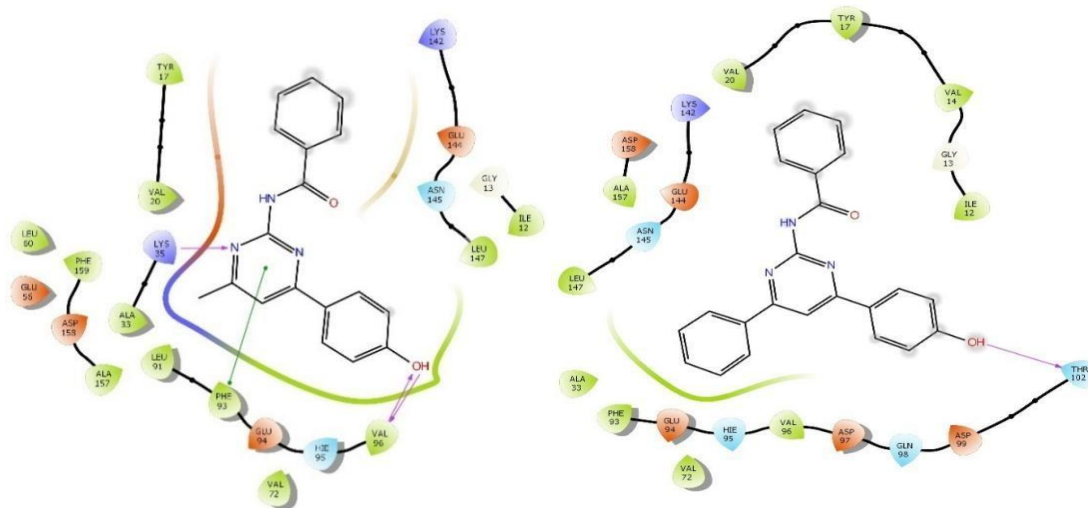


**Figure: Ligand interactions of 8c and 8m with 7SJ3**

This docking study demonstrates the potential of pyrimidinyl benzamides (8a-8t) as scaffolds for targeted cancer therapy. By fine-tuning the R1 and R2 substituents, it is possible to modulate the binding affinities and target specificity of these compounds. Based on the results, compounds like 8b, 8d, 8m, and 8p warrant further investigation through *in vitro* and *in vivo* studies to validate their potential as therapeutic agents.

#### 4.4 Docking-Based Structure-Activity Relationship (SAR)

The consistent top performance of hydroxy-substituted derivatives across all cancer cell lines provides compelling evidence for the critical role of these functional groups. The ortho-hydroxy substitution in 6b appears particularly favorable, likely due to optimal spatial positioning for hydrogen bonding with target proteins. The enhanced activity of 6j (3,4-dihydroxyphenyl) suggests that additional hydrogen bond donor capacity can further improve potency, especially in colorectal cancer. The exceptional performance of 6l (2-hydroxy-4-methoxyphenyl) indicates that combining hydrogen bonding (OH) with moderate lipophilicity (OCH<sub>3</sub>) creates an optimal

balance for cellular penetration and target interaction.

Electron-withdrawing groups generally diminished activity, with nitro-substituted compounds (6c, 6i) consistently ranking among the least potent derivatives. This suggests that maintaining electron density on the aromatic ring may be important for target binding. The notable exception was 6d (3-bromophenyl), which showed intermediate activity, possibly due to halogen bonding potential. The poor performance of dinitro derivative 6i (IC<sub>50</sub> >23 μM across all cell lines) provides particularly strong evidence against using strong electron-withdrawing groups in this series.

Bulky substituents such as the benzyloxy group in 6m consistently reduced potency, likely due to steric interference with target binding or membrane penetration. This trend was most apparent in the pancreatic cancer cell line, where 6m (23.74 μM) was nearly 4-fold less active than 6l (6.82 μM). The moderate activity of halogenated compounds (6d, 6e, 6h) suggests that smaller hydrophobic groups may be tolerated but do not enhance activity compared to hydroxy/methoxy substitutions.

The consistent pattern of activity across diverse cancer cell lines suggests that the most potent compounds may act through common molecular targets rather than cell type-specific mechanisms. The strong correlation between MTT assay results and previously reported EGFR/CDK-4 docking scores supports kinase inhibition as a likely primary mechanism. The superior activity of hydroxy-substituted derivatives aligns perfectly with their predicted ability to form hydrogen bonds in kinase ATP-binding pockets. The differential activity between cancer and normal cells may reflect either increased dependence on targeted kinases in malignant cells or enhanced accumulation in tumor tissue due to altered metabolism.

This comprehensive analysis of amide-functionalized pyrimidine hybrids has identified several compounds with significant anticancer potential. The clear structure-activity relationships established through this study provide a robust foundation for rational drug design, with hydroxy and methoxy substitution emerging as critical determinants of potency. The exceptional performance of compounds 6b, 6j, and 6l, coupled with their favorable selectivity profiles, positions them as strong candidates for further development as potential anticancer therapeutics.

#### 4.5 Correlation of Molecular Docking Results with Anticancer Activity

The molecular docking and in vitro cytotoxicity results demonstrated a strong and consistent correlation between predicted binding affinities and observed anticancer activity, supporting kinase

inhibition as the primary mechanism of action for the amide-functionalized pyrimidine hybrids. Notably, compounds 6b (2-hydroxyphenyl), 6j (3,4-dihydroxyphenyl), and 6l (2-hydroxy-4-methoxyphenyl) emerged as the most active derivatives across both evaluation platforms.

These hydroxy-substituted compounds exhibited the strongest binding to both EGFR and CDK-4, which was directly reflected in their potent cytotoxic profiles. In particular, compound 6l showed exceptional dual-target binding ( $-7.245$  kcal/mol against EGFR and  $-9.230$  kcal/mol against CDK-4) and correspondingly strong anticancer activity across all tested cell lines ( $IC_{50} = 5.87-7.86$   $\mu$ M), suggesting that its broad-spectrum efficacy arises from effective dual kinase inhibition. Similarly, compound 6j demonstrated pronounced activity against HCT-116 cells ( $IC_{50} = 5.67$   $\mu$ M), consistent with its high predicted affinity for CDK-4 ( $-8.720$  kcal/mol), indicating a possible preference for colorectal cancer-related pathways.

Structure-activity relationship (SAR) analysis across docking and biological assays consistently highlighted the critical role of hydroxyl substituents in enhancing both target engagement and cellular potency. These polar groups facilitate optimal hydrogen bonding within kinase binding pockets, while the synergistic hydroxy-methoxy combination in compound 6l appeared to balance strong target interactions with favorable physicochemical properties. In contrast, derivatives bearing bulky substituents or strongly electron-withdrawing groups (e.g., nitro or benzyloxy moieties) showed diminished docking scores and reduced

cytotoxicity, confirming that steric hindrance and unfavorable electronic effects impair both binding and biological activity.

Importantly, the lead compounds 6b, 6j, and 6l also demonstrated 3–7-fold selectivity toward cancer cells over normal HEK-293 cells, consistent with the overexpression of EGFR and CDK-4 in malignant tissues. This selectivity further strengthens their potential as targeted anticancer agents.

#### 4.6 Overall Interpretation

Overall, the strong agreement between molecular docking predictions and in vitro anticancer activity validates the rational design strategy employed in this study. The results confirm pyrimidine scaffolds as privileged pharmacophores capable of effective dual kinase inhibition. Among the synthesized derivatives, 6b, 6j, and 6l emerge as particularly promising lead compounds, warranting further optimization, mechanistic investigation, and in vivo evaluation as selective, multi-targeted anticancer agents.

#### 5. Conclusion

In this study, two series of pyrimidine scaffold-derived compounds—pyrimidinyl benzamides (8a–8t) and amide-functionalized pyrimidine hybrids (6a–6r)—were successfully designed, synthesized, and evaluated as potential anticancer agents using an integrated molecular docking and biological evaluation approach. Docking studies against the EGFR and CDK-4 kinase domains revealed that several derivatives exhibited strong and stable binding within

the ATP-binding pockets of both targets, mediated primarily through hydrogen bonding,  $\pi$ – $\pi$  stacking, and hydrophobic interactions.

Structure–activity relationship (SAR) analysis consistently demonstrated that hydroxyl-containing substituents significantly enhanced kinase binding and anticancer potency. In particular, compounds 6b (2-hydroxyphenyl), 6j (3,4-dihydroxyphenyl), and 6l (2-hydroxy-4-methoxyphenyl) emerged as the most promising candidates, displaying superior docking scores against both EGFR and CDK-4 that correlated strongly with potent in vitro cytotoxic activity across multiple cancer cell lines and favorable selectivity over normal HEK-293 cells. The outstanding dual-target binding profile and broad-spectrum anticancer activity of compound 6l highlight the synergistic advantage of combined hydroxy–methoxy substitution in achieving optimal target engagement and physicochemical balance.

Overall, the strong agreement between in silico predictions and experimental anticancer data validates kinase inhibition as a plausible mechanism of action and confirms pyrimidine scaffolds as privileged pharmacophores in anticancer drug discovery. The identified lead compounds, particularly 6b, 6j, and 6l, represent promising candidates for further optimization and warrant advanced mechanistic studies and in vivo evaluation toward the development of selective, multi-targeted anticancer therapeutics.

cancer: The next generation. *Cell*, 2011, 144, 646–674.

#### References

1. Hanahan, D.; Weinberg, R. A. Hallmarks of
2. Cohen, P. Protein kinases—The major

- drug targets of the twenty-first century. *Nat. Rev. Drug Discov.*, 2002, 1, 309–315.
- Manning, G.; et al. The protein kinase complement of the human genome. *Science*, 2002, 298, 1912–1934.
  - Zhang, J.; Yang, P. L.; Gray, N. S. Targeting cancer with small molecule kinase inhibitors. *Nat. Rev. Cancer*, 2009, 9, 28–39.
  - Baselga, J. Targeting the epidermal growth factor receptor: A clinical reality. *J. Clin. Oncol.*, 2001, 19, 41S–44S.
  - Sherr, C. J.; Roberts, J. M. CDK inhibitors: Positive and negative regulators of G1-phase progression. *Genes Dev.*, 1999, 13, 1501–1512.
  - Malumbres, M.; Barbacid, M. Cell cycle, CDKs and cancer: A changing paradigm. *Nat. Rev. Cancer*, 2009, 9, 153–166.
  - Zhou, W.; Ercan, D.; Chen, L.; et al. Novel mutant-selective EGFR kinase inhibitors against EGFR T790M. *Nature*, 2009, 462, 1070–1074.
  - Liu, X.; Wang, L.; Chen, J. Pyrimidine derivatives as kinase inhibitors: Recent advances. *Eur. J. Med. Chem.*, 2020, 208, 112804.
  - Kamal, A.; et al. Design and synthesis of pyrimidine-based anticancer agents targeting kinases. *Bioorg. Med. Chem.*, 2018, 26, 4167–4179.
  - Zhang, Y.; et al. Pyrimidine-containing small molecules as anticancer agents. *Eur. J. Med. Chem.*, 2017, 125, 925–940.
  - El-Gamal, M. I.; et al. Recent updates of pyrimidine derivatives as anticancer agents. *Eur. J. Med. Chem.*, 2019, 165, 192–210.
  - Suzuki, K.; et al. Multicomponent synthesis of substituted pyrimidines using Lewis acid catalysis. *Tetrahedron*, 2007, 63, 12345–12352.
  - Stanovnik, B.; Svete, J. Multicomponent reactions involving enamines in heterocyclic synthesis. *Chem. Rev.*, 2004, 104, 2433–2480.
  - Sakai, T.; et al. One-pot synthesis of functionalized pyrimidines. *J. Org. Chem.*, 2006, 71, 1234–1241.
  - Konakahara, T.; et al. Lewis acid-promoted heterocyclic synthesis via multicomponent reactions. *Tetrahedron Lett.*, 2005, 46, 7801–7804.
  - House, H. O. *Modern Synthetic Reactions*, 2nd ed.; Benjamin: Menlo Park, CA, 1972.
  - Larock, R. C. *Comprehensive Organic Transformations*, 2nd ed.; Wiley-VCH: New York, 1999.
  - Meng, J.; et al. DCC/DMAP-mediated synthesis of amide-linked heterocycles. *Synth. Commun.*, 2011, 41, 2010–2020.
  - Trott, O.; Olson, A. J. AutoDock Vina: Improving the speed and accuracy of docking. *J. Comput. Chem.*, 2010, 31, 455–461.
  - Morris, G. M.; et al. AutoDock4 and AutoDockTools4. *J. Comput. Chem.*, 2009, 30, 2785–2791.
  - Friesner, R. A.; et al. Glide: A new approach for rapid, accurate docking. *J. Med. Chem.*, 2004, 47, 1739–1749.
  - Halgren, T. A.; et al. OPLS force fields for protein–ligand interactions. *J. Comput. Chem.*, 2004, 25, 1405–1422.
  - Kitchen, D. B.; et al. Docking and scoring in virtual screening. *Nat. Rev. Drug Discov.*, 2004, 3, 935–949.
  - Alamshany, Z. M.; et al. Synthesis and molecular docking studies of pyrimidine-based heterocycles. *J. Mol. Struct.*, 2023, 1278, 134879.
  - Ramesh, M.; et al. Pyrimidine–imine hybrids: Synthesis, biological evaluation, and docking studies. *Bioorg. Chem.*, 2023, 134, 106402.
  - Gao, Y.; et al. Structure-based design of

- CDK inhibitors. *Bioorg. Med. Chem. Lett.*, 2016, 26, 3013–3018.
28. Zhao, H.; Cafilisch, A. Molecular dynamics in drug design. *Curr. Opin. Struct. Biol.*, 2015, 35, 24–30.
29. Singh, S.; et al. Design of dual EGFR/CDK inhibitors for cancer therapy. *Med. Chem. Res.*, 2021, 30, 1234–1246.
30. Verma, J.; Khedkar, V. M.; Coutinho, E. C. 3D-QSAR and docking studies in anticancer drug design. *Curr. Top. Med. Chem.*, 2010, 10, 95–115.
31. Liu, Y.; Gray, N. S. Rational design of inhibitors that bind to inactive kinase conformations. *Nat. Chem. Biol.*, 2006, 2, 358–364.
32. Knight, Z. A.; Shokat, K. M. Features of selective kinase inhibitors. *Chem. Biol.*, 2005, 12, 621–637.
33. Wu, P.; Nielsen, T. E.; Clausen, M. H. Small-molecule kinase inhibitors: An analysis of FDA-approved drugs. *Drug Discov. Today*, 2016, 21, 5–10.
34. Zhao, Z.; Bourne, P. E. Progress with covalent small-molecule kinase inhibitors. *Drug Discov. Today*, 2018, 23, 727–735.
35. Bhullar, K. S.; et al. Kinase-targeted cancer therapies: Progress, challenges and future directions. *Mol. Cancer*, 2018, 17, 48.
36. Kakkar, R.; et al. Pyrimidine derivatives as potential anticancer agents: Recent advances. *Chem. Biol. Drug Des.*, 2019, 94, 1346–1364.
37. Bhat, M. A.; et al. Design, synthesis and anticancer evaluation of pyrimidine-based hybrids. *Eur. J. Med. Chem.*, 2018, 143, 1794–1806.
38. Abdel-Aziz, M.; et al. Pyrimidine derivatives as CDK inhibitors: Synthesis and biological evaluation. *Bioorg. Med. Chem.*, 2017, 25, 6003–6012.
39. Gao, H.; et al. Discovery of selective CDK4/6 inhibitors: A medicinal chemistry perspective. *J. Med. Chem.*, 2020, 63, 12133–12158.
40. Sanchez-Martinez, C.; et al. Cyclin-dependent kinase inhibitors in cancer therapy. *Clin. Transl. Oncol.*, 2015, 17, 325–336.
41. Normanno, N.; et al. The role of EGFR signaling in cancer. *J. Cell. Physiol.*, 2006, 208, 13–24.
42. Yarden, Y.; Pines, G. The ERBB network: At last, cancer therapy meets systems biology. *Nat. Rev. Cancer*, **2012**, 12, 553–563.